29

FERMILAB
JAN 14 1999
LIBRARY

STEWARD-1461

PREPRINTS

of the

STEWARD OBSERVATORY

THE UNIVERSITY OF ARIZONA
TUCSON, ARIZONA 85721-0065 U.S.A.

Fermilab Library
0 1160 0062213 8

No. 1461

THE POLARIZATION OF BALQSOs[1]

GARY D. SCHMIDT AND DEAN C. HINES[2]
Steward Observatory, The University of Arizona, Tucson, AZ 85721, U.S.A.
gschmidt@as.arizona.edu, dhines@as.arizona.edu

NAME | I.D No. | M.S.
RETURN TO FERMILAB

TO APPEAR IN THE ASTROPHYSICAL JOURNAL, PART 1

[1]A portion of the data presented here were obtained with the facilities of the National Optical Astronomy Observatories, which is operated by the Association of Universities for Research in Astronomy, Inc., under contract with the National Science Foundation.

[2]Guest Observer, McDonald Observatory, The University of Texas at Austin

THE POLARIZATION OF BALQSOs[1]

Gary D. Schmidt and Dean C. Hines,[2]
Steward Observatory, The University of Arizona, Tucson, AZ 85721
gschmidt@as.arizona.edu, dhines@as.arizona.edu

ABSTRACT

We present the combined results of optical polarization surveys of QSOs showing broad absorption lines (BALQSOs) conducted at the Steward and McDonald Observatories. The merged list of 53 objects provides the first statistical justification for claims of the tendency of BALQSOs to show stronger-than-average polarization, with a typical BALQSO being polarized a factor 2.4× greater than a QSO from an optical survey selected without regard for absorption lines. Spectropolarimetry of sufficient quality to distinguish the polarization of emission lines *vs.* absorption troughs *vs.* continuum is also presented for 6 objects from the survey. When taken together with published data on other sources, the results lead to several significant correlations which can be used to gain insight into the structure of a BALQSO. These include: 1) a reduced degree of polarization in the broad emission lines; 2) enhanced polarization in the absorption troughs; and 3) an increase in the degree of polarization toward shorter wavelengths. In addition, BALQSOs with more prominent absorption systems tend to be more strongly polarized, and there is evidence that the subclass of low-ionization absorbers is more strongly polarized than other BALQSOs. If the increased polarization of BALQSOs is due to attenuation of direct, as opposed to scattered, lines of sight to the nucleus, absorption-line objects are underrepresented in optical surveys and their true incidence is 20%–30% that of all UV-bright QSOs. Nevertheless, BALQSOs on average are not as highly polarized as their more obscured radio-quiet cousins, the *IRAS*-QSOs/Hyperluminous Infrared Galaxies. We are led to a consistent picture in which broad absorption is observed in BALQSOs because they are inclined at intermediate inclinations where our line of sight passes through gas clouds located near the surface of a dusty torus.

Subject headings: polarization — quasars:absorption lines — quasars:emission lines — quasars:general

---

[1]A portion of the data presented here were obtained with the facilities of the National Optical Astronomy Observatories, which is operated by the Association of Universities for Research in Astronomy, Inc., under contract with the National Science Foundation.

[2]Guest Observer, McDonald Observatory, The University of Texas at Austin

1. INTRODUCTION

Interest in the polarization of the so-called Broad Absorption Line QSOs (BALQSOs) dates to the discovery of the prototype PHL 5200 (Lynds 1967). Because the absorption features are associated with resonance transitions that are typically also seen strongly in emission, it was recognized (Scargle, Caroff, & Noerdlinger 1970) that the polarization of the features contains potential information on the structure of the emitting and absorbing regions. These discussions predated accurate polarization surveys of QSOs. The observations of Stockman & Angel (1978) and Moore & Stockman (1984) found that QSOs could be divided polarimetrically into two nearly disjoint groups: "normal" QSOs (termed Low-Polarization QSOs or LPQs), with $P \lesssim 2\%$; and High-Polarization QSOs (HPQs), which by definition must exhibit $P > 3\%$. The latter are very often identified with sources of the Blazar class, whose strong and highly variable polarization is attributed to synchrotron emission from a relativistically-enhanced jet beamed nearly along our line of sight. Indeed, a complete polarization survey of the Palomar Green catalog of objects whose broadband colors match those of a typical unbeamed QSO found no highly-polarized QSOs among 114 objects (Berriman et al. 1990).

Moore & Stockman (1984) pointed out that only two radio-quiet, non-variable QSOs from their survey of 239 targets exceeded the polarization threshold for a highly-polarized object. Both were BALQSOs (PHL 5200 and H1413+117). This, plus the stronger-than-average polarization of several other BALQSOs in their sample refocused attention on the polarization of the class. However, spectropolarimetry of PHL 5200 by Stockman, Angel, & Hier (1981) found that the C IV λ1550 emission line exhibited *weaker* polarization than the surrounding continuum (and much weaker than the absorption feature), in contradiction to the resonance-scattering model of Scargle et al. (1970).

More recently, spectropolarimetry has provided a fresh view into the structure of AGN and into the role that viewing perspective plays in object classification. The discovery of polarized, scattered, broad emission lines from the Seyfert 2 galaxy NGC 1068 (Antonucci & Miller 1985) and subsequently in other radio-quiet and -loud AGN of moderate luminosity (see Antonucci 1993 for a review) strongly suggests the existence of an opaque, possibly toroidal structure which obscures the nuclear continuum source and compact broad emission-line region (BELR) when viewed at high inclination. Images of ionized regions with conical morphology apparently illuminated through the hole of a torus (e.g., Macchetto et al. 1994) and of dusty toroidal disks in nearby examples (Jaffe et al. 1996) further support this general picture. Finally, it has recently become apparent that at least some of the missing "QSO 2s" – high-luminosity analogues of the Type 2 Seyferts – can be found among the most IR-luminous active galaxies discovered by *IRAS*. These *IRAS*-QSOs/Hyperluminous Infrared Galaxies (Cutri et al. 1994: Low & Hines 1998) often reveal highly-polarized, scattered broad emission components underlying their tremendous narrow permitted-line spectra (e.g., Hines & Wills 1993; Hines et al. 1995; Young et al. 1996). Thus, the "unification" offered by the obscuring torus model appears to transcend both luminosity and spectral class.

In the context of this unified scheme for radio-quiet AGN, attention has returned to BALQSOs as possible "transition objects" between the classical QSOs, which are interpreted as objects seen at low inclination, and the more edge-on examples. Detailed spectropolarimetry of certain strongly-polarized BALQSOs (e.g., Glenn, Schmidt, & Foltz 1994; Hines & Wills 1995; Goodrich & Miller 1995; Cohen et al. 1995) have been interpreted successfully in terms of a view which grazes the surface of an obscuring structure, and where ablation of clouds from that surface produces the observed absorption features (Weymann et al. 1991, hereafter WMFH; Voit, Weymann, & Korista 1993). However, despite these clues, the quest for an overall picture has not been grounded in a statistical justification for BALQSOs representing a class with intermediate polarization, and we have not seen detailed spectropolarimetric analyses of a significant sample of objects.

2. THE SURVEY

During the period 1978–1995, two polarimetric surveys of BALQSOs were carried out at Steward Observatory, The University of Arizona and McDonald Observatory of The University of Texas. The measurements were made in nearly identical wavebands and with similar sensitivities using several generations of polarimeter at Steward Observatory of both the Pockels cell and rotating waveplate variety, and with the Breger polarimeter at McDonald (Breger 1977; Wills et al. 1992a). The initial observation of each object was always obtained in "white" light ($\lambda\lambda 3200 \sim 8600$) but on occasion defined spectral bands were added to study the wavelength dependence of polarization. The combined results of the two surveys are presented in Table 1 in the following column order: object designation and emission redshift (as listed by Sowinski, Schmidt, & Hines 1997), date of observation, telescope used, waveband, degree of polarization and uncertainty, and finally polarization position angle and uncertainty. From an inspection of data for objects with multiple measurements there is no convincing evidence for time variability, nor is there any indication of significant systematic differences between the results for the two observatories. Thus, for these objects the white-light observations were combined as an error weighted mean of the normalized Stokes parameters. This best estimate of the polarization is contained as an additional entry in the table. The degree of polarization listed is as measured, without any correction for bias, and the position angle uncertainty in degrees is estimated as $\min(28.65\sigma_P/P, 52)$ as suggested by Wardle & Kronberg (1974). Neither of these approximations is of importance as long as we confine ourselves to high S/N, i.e. $P/\sigma_P \gtrsim 4$ (Simmons & Stewart 1985).

The combined Steward/McDonald survey comprises 53 BALQSOs which have been cataloged as showing definite or probable absorption associated with the host object. Data quality varies with object brightness, telescope size, and duration of the observation, so that uncertainties in the coadded white-light polarization range $\sigma_P = 0.08\% - 1.75\%$. Nevertheless, 32 objects have $\sigma_P \leq 0.5\%$, and the mean for the entire sample, $\langle\sigma_P\rangle = 0.48\%$, is sufficiently small to yield a 4σ detection for $P \sim 2\%$ and efficiently discriminate high-polarization sources from the

run-of-the-mill QSO. Figure 1 compares the differential and cumulative polarization distributions for the BALQSO sample with the optically-selected[3] Palomar-Green (PG) survey (Schmidt & Green 1983) as measured by Berriman et al. (1990).

Both Berriman et al. and Moore & Stockman (1984) went to considerable effort to show that the small but significant polarizations measured for their samples could not arise by the interstellar mechanism in our Galaxy. Our BALQSO sample is even more immune to this problem. Not only do the objects measured comprise an overwhelmingly high-latitude sample (half have $b^{II} > 60°$ and 90% have $b^{II} > 45°$), their mean polarization is much larger: $\langle P \rangle_{\rm BALQSO} = 1.26\%$ *vs.* $\langle P \rangle_{\rm PGQSO} = 0.53\%$ for the PG distribution. Finally, the strong polarization differences between the lines and continua for the objects studied by spectropolarimetry (§3) prove that interstellar polarization cannot be a significant component for at least the strongly polarized objects.

Half of the 53 BALQSOs are polarized above 1%, and 8 exceed $P = 2\%$. These numbers are to be compared with 12 and 2 of the 114 PG QSOs, respectively. A two-tailed K-S test of the two distributions yields a probability of only 3×10^{-7} that two samples of these sizes drawn from the same parent would differ by as much or more than is seen in Figure 1. It is true that because of brightness differences for the two catalogs the uncertainty distributions differ: $\langle \sigma_P \rangle = 0.48\%$ for the BALQSOs *vs.* $\langle \sigma_P \rangle = 0.17\%$ for the PG QSOs, but the mean polarization of the 32 BALQSOs with $\sigma_P \leq 0.5\%$ is very similar to that of the 21 less well-measured objects, $\langle P \rangle = 1.41\%$ *vs.* 1.02%, and the K-S probability of the null hypothesis for these BALQSO subsamples is 0.72. Thus, the positive polarization bias lent by the finite uncertainties appears to not significantly affect the statistical distributions. The inference of Moore & Stockman (1984) that BALQSOs as a class tend to be more strongly polarized than other radio-quiet QSOs is conclusively established.

3. SPECTROPOLARIMETRY OF 6 BALQSOs

Beginning with CSO 755 (1524+5147; Glenn et al. 1994), spectropolarimetric observations were carried out at Steward Observatory for several of the more strongly polarized objects in an effort to gain insight to the origin of polarization and structure of these objects. The data were acquired with the CCD Spectropolarimeter described by Schmidt, Stockman, & Smith (1992) attached to the 2.3 m Bok telescope on Kitt Peak. In 1993, a 1200×800 pixel LORAL CCD replaced the original Texas Instruments device, providing the bulk of the data with a spectral coverage of $\sim\lambda\lambda 4000 - 8000$ (observer's frame) and resolution of $\sim$12 Å. Each object was observed for a total of 3–6 hr divided among $\sim$3 epochs during the years 1991–1995. Typically, the 3″-wide slit used easily accomodated the seeing profile. Polarimetric calibrations were applied for each observing run based on observations of a bright target through a fully-polarizing prism and of

[3]Radio-loud objects are rare among current samples of BALQSOs (Stocke et al. 1992; Becker et al. 1997; cf. Brotherton et al. 1998).

polarization standard stars from the list of Schmidt, Elston, & Lupie (1992). Calibration of total spectral flux was based on standard stars from the various *IRAF* databases, observed each night with the same instrumental setups. Again, no significant differences were apparent among the spectrum-added polarization values for a given QSO, so the data were coadded as Stokes vectors to overall means weighted according to the statistical quality of each epoch.

The spectropolarimetric results for the BALQSOs 0226−1024, 0932+501, 1246−057, 1413+117, 0759+6508, and 1700+518 are presented in Figures 2–7 as plots of the total spectral flux F_λ, polarized (Stokes) flux $q' \times F_\lambda$, degree of polarization P, and position angle θ. Some of these data have previously been displayed by Schmidt, Hines, & Smith (1997)[4].

The objects chosen for spectropolarimetry span the redshift range $z = 0.148$ for 0759+6508 to 2.551 for 1413+117. Though generally selected for their large polarization, $1.0\% \lesssim P \lesssim 2.5\%$, the aperture of a 2.3 m telescope is simply insufficient to provide detailed, high S/N polarization spectra for the fainter objects ($V \gtrsim 17$). Our goal here is not to compete with the exquisite data which are now beginning to appear from the world's largest telescopes. Instead, we seek to identify trends and common characteristics among a sample of sufficient size to gain information on the generic structure of a BALQSO. We begin with a few notes regarding the individual objects.

0226−1024 The high-redshift examples place the C IV λ1550 resonance doublet, C III] λ1909, and occasionally Lyα in our region of sensitivity. The absorption spectrum of 0226−1024 is unusually complex below C IV λ1550, showing at least 4 systems between −2000 km s^{-1} and −30,000 km s^{-1} of the emission lines. The continuum polarization is ~2%, and increases mildly to the blue ($P_\lambda \propto \lambda^{-0.4}$; uncertainties in these spectral indices are 0.1 – 0.2). From inspection of the polarized flux spectrum in Figure 2, it is clear that the BELs of 0226−1024 do not share the polarization of the continuum. The degree of polarization increases strongly in the principal BAL features, approaching $P = 10\%$ in the deepest trough. However, the absorbed light cannot be simply dilution, since the troughs are also seen in Stokes flux. These conclusions are confirmed at higher S/N by Ogle (1997), who also notes the lack of a polarization feature in the least-displaced trough and a slight rotation of θ in others.

0932+501 Though not polarized as strongly as some of the other examples, ($P_{cont} = 1.5\%$), the wavelength dependence of polarization of 0932+501 (Figure 3) is the steepest of the sample studied, with $P_\lambda \propto \lambda^{-0.9}$. The significance of this may extend to the fact that 0932+501 is a low-ionization BALQSO (Mg II-Al III absorber). Sprayberry & Foltz (1992) have found that these objects as a class show energy distributions significantly affected by dust. The BEL flux of 0932+501 is apparently unpolarized, but P is enhanced in at least the low-velocity C IV λ1550 trough. A rotation of −20° in θ occurs from 1400 Å to 2500 Å rest.

[4]Note that Figure 2 of that paper suffers from mislabeling of the $P(\%)$ axis and line identifications for 1413+117.

1246−057 The data for 1246−057 shown in Figure 4 follow the trends suggested by the previous objects, with unpolarized emission lines and a dramatic increase in P in the C IV λ1550 trough. Despite a total integration time less than for any of the other faint BALQSOs, a slight increase in polarization to the blue is indicated, $P_\lambda \propto \lambda^{-0.1}$. The position angle is essentially constant at $\theta = 139°$ throughout.

1413+117 (The Clover Leaf QSO) The polarization of 1413+117 (Figure 5) differs from the remainder of our sample by showing only a *partial* reduction in the emission line of C IV λ1550 and apparently also at Lyα. The BAL troughs associated with these features and with the Si IV λ1397 doublet are all strongly polarized and overall the Stokes flux is slightly bluer than the total flux spectrum, with $P_\lambda \propto \lambda^{-0.3}$. Goodrich & Miller (1995) reached similar conclusions, but also noted time variability in both P and θ and at some epochs differences between the polarization position angle of emission or absorption lines and the continuum. This may be related to the fact that 1413+117 is a multi-image lensed object (e.g., Turnshek et al. 1997b and references therein). Our data were taken within the 4-month period 1993 Feb. through 1993 June (JD 2449045−2449160), and are in good agreement with pre-1994 data of Goodrich & Miller (their Table 1 and Figure 2). With our short baseline of only 4 months, no new information is provided on the time variability, however significant rotations in θ appear to occur in the wings of the major absorption troughs. The cores of the troughs are sufficiently black that position angles here are undetermined.

0759+6508 and 1700+518 These two low-z examples offer no strong resonance troughs in our spectral window, but the polarization spectra presented in Figures 6 and 7 nevertheless hold clues to their nuclear structure. The dominant emission line, Hα, displays a clear change in P across its profile in both objects. For 0759+6508, the line flux appears to largely dilute a polarized continuum, but a 20° rotation in θ across the profile attests to weak intrinsic polarization. At a $b^{II} = 32.5°$, this may be the only object in our spectropolarimetric sample where the interstellar mechanism is important. Broadband measurements of stars in the vicinity suggest that $P_{\rm IS} = 0.33\%$, $\theta_{\rm IS} = 7°$ (B. Wills, private communication), much weaker than the ~0.75% value required to eliminate the Hα position angle rotation. At this time the interstellar component toward 0759+6508 remains in question. Nevertheless, for any assumed interstellar component, there exists a significant rotation in θ across the spectrum and a large amount of the structure in the spectrum of P remains. The latter can be attributed to dilution by other permitted lines, esp. Hβ and Fe II multiplets. Both 0759+6508 and 1700+518 are low-ionization BALQSOs, with the former showing an increased degree of polarization at the Na I λ5890, 96 absorption doublet (Hines & Wills 1995). A corresponding broad peak in P is also present in our lower resolution data. The smooth spectrum of Stokes flux across this region suggests that the absorbed light may be unpolarized. In 1700+518, $\mathcal{S}$-waves are seen in P, Stokes flux, and θ at each of the major emission lines. Clearly, this is an example where the polarizing mechanism "sees" a different geometry for red- *vs.* blue-shifted BEL clouds. A rotation of ~10° in θ through the spectrum is also significant.

The degree of polarization increases very mildly to the blue in both examples, with $P_\lambda \propto \lambda^{-0.2}$.

The above objects bring to a total of 11 the number of BALQSOs for which spectropolarimetry is now available. The aforementioned CSO 755 (1524+5147) displayed for the first time polarization differences of the BAL features from the emission lines and continuum (Glenn et al. 1994). The original observations of PHL 5200 (Stockman et al. 1981) have now been superseded by accurate data from Goodrich & Miller (1995) and Cohen et al. (1995); the latter authors also present results for 0105−265. Finally, high-quality data on the low-ionization/radio source 0840+3633 has recently been reported by Brotherton et al. (1997) and the strongly-polarized BALQSO IRAS 14026+4341 is discussed by Hines et al. (1998c). To this list might also be added the Seyfert 1 galaxy Mk 231, which contains (narrow) displaced absorption features of several low-ionization species and polarization structure across its broad emission lines very similar to that seen in 1700+518 (Smith et al. 1995).

4. CORRELATIONS AND TRENDS

With 53 objects observed for polarization, it is possible to examine the data for trends that might lend clues to the structural properties and polarizing mechanism(s) of BALQSOs. To the extent that BALQSOs might well represent a geometrically-selected sample of all (radio-quiet) QSOs, such as one viewed from high inclination (e.g., WMFH), these conclusions will be useful for understanding the general QSO phenomenon. In discussing these characteristics below, we refer the reader to Table 2, where several trends identified among the spectropolarimetric subsample are summarized.

4.1. Enhanced Polarization of BALQSOs

The foremost trait of the polarization of BALQSOs is that described in §2: their marked tendency to be more strongly polarized than the typical radio-quiet QSO. This applies not only to extreme cases like PHL5200 and 1402+4341 (which reaches a U-band polarization of more than 14%), but the mean polarization of the BALQSO sample is 2.4× higher than that of the PG catalog. The lack of variability and significant emission-line polarization of some examples argue against synchrotron emission as the general polarizing mechanism; instead authors have universally borrowed from the unification ideas successfully applied to Seyfert and radio galaxies by invoking small-particle scattering in the vicinity of the nucleus. The interpretation of BALQSOs, then, is that these objects tend to present more extensive scattering media and/or extreme geometries to our line of sight compared with typical UV-bright QSOs.

Does the broad-band polarization of BALQSOs suggest a uniform set, or are there trends within the sample? Two characteristics which have been used to subdivide BALQSOs are the balnicity index of WMFH – basically a measure of the depth and extent of absorption – and the

presence or absence of BAL features associated with low-ionization lines. In Figure 8 is displayed the relationship between white-light polarization and C IV λ1550 balnicity index for the 33 survey objects which are in common with the samples of WMFH and Korista et al. (1993)[5]. While there is considerable scatter in the diagram, a positive trend between P and balnicity index is indicated. The linear correlation coefficient $r = 0.37$ for a linear fit implies a likelihood of $\sim$5% that such a correlation would be obtained by chance. Points labeled with filled squares represent members of WMFH's "Sample 9" – the low-ionization BALQSOs. Though the sample is small, these objects tend to be found both at higher balnicity index and higher polarization than the norm. A K-S test comparing all known low-ionization BALQSOs from our survey (10 objects) with the remaining 43 indicates a probability of about 10% – a 2σ result – that the two groups would be drawn at random from the same parent. Not only are BALQSOs polarized on average to a greater degree than non-BALQSOs, but within the BALQSO class, it appears that polarization tends to increase with the increased presence and range of ionization of the absorbing material.

4.2. Reduced Polarization in the Emission Lines

A trait common to all of the BALQSOs studied by spectropolarimetry is a decrease in degree of polarization at the locations of the BELs. Stokes flux spectra generally show no sign of the emission lines, indicating that the reduction is often total. The inference is that the scattering region cannot be significantly larger than the BELR, and may in fact be coincident with it. In 1413+117, C IV λ1550, Si IV λ1397, and C III] λ1909 appear with reduced equivalent widths in the spectrum of Stokes flux (see also Goodrich & Miller 1995). Here, the scatterers presumably extend further out. A complication to the interpretation of emission-line polarizations is the possibility of intrinsic polarization due to resonance scattering *within the BELR*. In this case, the polarization position angle in the line might be used to infer the direction of elongation of the emission region. Weak polarization of the C III] line alone has been observed in PHL 5200 (Goodrich & Miller 1995; Cohen et al. 1995); the process can be important for a semiforbidden line but not likely for the far higher optical depths encountered by permitted lines (Cohen et al. 1995; Blandford & Lee 1997 and references therein).

4.3. Enhanced Polarization in the Absorption Troughs

A tendency toward an increased degree of polarization in the BAL troughs is also shared by every object studied thus far. This has generally been interpreted to indicate decreased dilution in the troughs, a consequence of the BAL clouds being more efficient at obscuring a compact nuclear

[5]The balnicity index is an equivalent width in units of km s^{-1} for those portions of contiguous absorption displaced more than 2000 km s^{-1} and for lines exceeding a threshold of 10% depth. Measurement of a balnicity index has not been systematically followed by subsequent authors.

source than the more extended scattering region. The degree of polarization observed in several of the troughs (e.g., 1413+117, 0226−1024) implies that the scattered component itself must be polarized by at least 10%! On the other hand, because the BALs are formed by resonant scattering as opposed to pure absorption, some polarized emission-line photons could be "redistributed" into the line wings and tend to fill in the troughs (e.g., Blandford & Lee 1997). The effect may have already been detected as polarization features in the red emission-line wings of 0226−1024 (Ogle 1997). Both 0226−1024 and CSO 755 (Glenn et al. 1994) exhibit a curious departure from the rule for the lowest-velocity troughs, where the degree of polarization is unchanged and hence BALs appear also in polarized flux. These objects earn a mixed designation in Table 2. In CSO 755, the low-velocity trough is actually situated $\sim$500 km s^{-1} to the red of emission-line center.

On purely spectroscopic grounds, it has long been clear that some troughs consume a considerable fraction of the blue emission-line wings (see review by Turnshek 1988), hence the absorbers must lie exterior to and cover solid angles as large as the BELR. The basic hierarchy for the nuclear components, in order of increasing radial distance, is therefore: *continuum source : scattering region : broad emission-line region : broad absorption-line region.*

4.4. Increase in Polarization toward Shorter Wavelengths

Without exception, the overall spectrum of polarized flux is bluer than that of total flux, as indicated by the run of $P_\lambda(\%)$ and recorded in Table 2. Expressed as a power law ($P_\lambda \propto \lambda^\beta$), the spectral index is not large, $-0.9 \lesssim \beta \lesssim -0.1$, but in no case is the wavelength dependence measured to be strictly flat. While low-redshift examples 1700+518 and 0759+6508 clearly show that Fe II emission lines can be important in some cases, detailed models of Keck data show that dilution by unpolarized Fe II emission cannot be the sole explanation (Ogle 1998). The trend might be interpreted to favor dust over electrons as the scattering particles, but the existence of dust within the BELR is debatable, and electron scattering coupled with wavelength-dependent dilution can also produce the observed results (e.g., Wills et al. 1992b). With multiple lines of sight playing an obvious role in forming the net spectrum of a polarized BALQSO, the combination of a neutral scattered component plus a more direct view which may be attenuated by outlying dust is an attractive possibility.

The sense of the wavelength dependence suggests that in a broadband survey, the degree of polarization should tend to correlate with redshift[6]. However, because BALs are associated with resonance lines, high-redshift objects dominate current catalogs and the results are extremely sensitive to the few low-z examples. Our survey actually shows an anticorrelation between polarization and redshift when all 53 objects are included, but the trend is strongly biased by the

[6]For characteristic equivalent widths, dilution by the generally unpolarized UV emission lines for a typical $z \sim 2$ BALQSO amounts to only 5%−10% in the "white-light" bandpass of the polarimetric survey.

enormous polarization of 1402+4341 ($P = 7.6\%$) at $z = 0.323$. This is an object selected from the *IRAS* Point Source Catalog for its high degree of obscuration, hence strong polarization was in some sense predetermined (Wills & Hines 1997). The limiting flux density of the PSC is too high to probe to the large redshifts typical of BALQSOs. To illustrate the fickleness of the test, the omission of just 1402+4341 inverts the dependence to a weak positive correlation, $P \propto (1+z)^{0.5}$. The latter slope is consistent with the typical wavelength dependence of polarization measured for the spectropolarimetric subset but the correlation coefficient is only $r = 0.2$. We believe that the use of white-light polarimetry for gaining insight into, e.g., the nature of the scattering particles is non-trivial at best.

5. DISCUSSION

5.1. Populations and Covering Factors

Polarization distributions of different classes of QSOs are important diagnostics for attempts to unravel the structure of the nuclear region and identify the various spectral components. Goodrich (1997a,b; see Krolik & Voit 1998 for an alternate view) has considered one variation on the model outlined in §1, in which he assumes that BALQSOs are a viewing-selected subset of all radio-quiet QSOs. The increased polarization of the absorption-line objects is assumed to be simply the result of attenuation along the direct (unscattered) line-of-sight to the nuclear continuum source. The attenuation factor (not necessarily simply absorption) is approximately the ratio of the characteristic polarizations of the two samples, $A \approx \langle P_{\rm BALQSO}\rangle / \langle P_{\rm non-BALQSO}\rangle$. Comparing our BALQSO sample and the PG QSOs, we have found $A = 2.4 \pm 0.3$ (§4.1). As shown in Figure 1, the two samples are indeed consistent with this hypothesis: a shift of the PG QSO sample by a factor 2.4 results in a modified distribution which is an excellent match to the observed BALQSO curve, and the 2-tailed K-S test reveals that the two distributions are then indistinguishable at the 98% confidence level.

In magnitude-limited samples, the amount of attenuation has important consequences for the "true" – as opposed to "observed" – fraction of QSOs which are absorption-line objects. For the simple case where a single attenuation factor applies to all BALQSOs, the assumption of Goodrich (1997a,b) that $A = 3 - 4$ implies that the observed fraction of BALQSOs is deficient by a factor[7] $4 \lesssim f(true)/f(obs) \lesssim 10$. Since typical estimates of $f(obs)$ are ~0.1 (Foltz et al. 1990), $A > 4$ would be unphysical and require modifications to the model. Our attenuation factor of $A = 2.4 \pm 0.3$ based on much-improved statistics corresponds to a correction factor in the range $2 - 3$, i.e. the space density of objects that exhibit BALs is 20%–30% that of all objects which would be classified as QSOs. Under the prescription of Weymann (1997), this quantity is known

[7] We correct a factor of ~2 error in Goodrich (1997a,b) due to his integrating, rather than averaging, the correction factor over z.

as the "global covering factor". Our range for this factor is consistent with estimates of Turnshek et al. (1997a) and Hamann, Korista, & Morris (1993) from completely different approaches.

Direct imaging of AGN indicates that, when scattering or ionization cones can be discerned, their extents are apparently defined by the escape of central continuum light through the dusty torus, and that the resulting half-opening angles of the cones fall in the range $30° < \theta_c < 60°$ (e.g., Wills et al. 1992b; Storchi-Bergmann, Wilson, & Baldwin 1992; Hines & Wills 1993; Hines et al. 1998b). This implies that as few as half of all luminous AGN are visible directly (through the "hole" of the donut) and classified as emission-line QSOs with strong broad lines. The remainder are obscured by the torus and seen as strong narrow-line sources with broad lines seen only in polarized light due to scattering. In addition, these objects have large values of $\log(L_{IR}/L_{opt})$ (Hines et al. 1995; see also below), and are identified at least in part with the *IRAS*-QSOs.

If a luminous AGN has a characteristic $\theta_c \lesssim 60°$ and BALQSOs represent transition objects seen at intermediate inclination, a BALQSO fraction of 0.2–0.3 can be interpreted to imply that the absorbing clouds occupy a "skin" of angular extent $\Delta\theta > 7°$ on the occulting torus. That is, if all QSOs are incipient BALQSOs, absorbing clouds occult the line of sight only for $53° \lesssim i \lesssim 60°$. The wedge could be thicker if the material is patchy enough that sightlines to the nucleus can miss BAL clouds even if observed from within the wedge. The geometry we are outlining is consistent with spectroscopic studies that appeal to large covering factors to account for the lower [O III] emission line strengths of BALQSOs compared with non-BALQSOs (e.g., Boroson & Meyers 1992; McIntosh et al. 1998). The confinement of BAL material to the skin of the torus and the accompanying attenuation along direct sightlines to the nucleus also address a potential problem with the unified scheme in explaining the apparently abrupt "turn-on" of high polarization with the presence of BALs (Goodrich 1997a). We note from the models of Brown & McLean (1977) that a uniformly-filled scattering cone with $\theta_c = 60°$ illuminated from its apex yields a degree of polarization to the scattered light $P > 10\%$ only for viewing inclinations of $i > 40°$. This polarization is about the maximum observed in the deep troughs of BALQSOs (§4.3), so we would expect to find BALQSOs only in this range of inclination, consistent with the location of the wedge estimated above. The ratio of ~50:50 in the space densities of QSOs and *IRAS*-QSOs implied by $\theta_c \sim 60°$ is also broadly consistent with the admittedly poor statistics of AGN with large $\log(L_{IR}/L_{opt})$ in the local universe (Low et al. 1988, 1989; Wills et al. 1992b).

5.2. Unification of (Radio-Quiet) QSOs

The continuity between *QSOs : BALQSOs : IRAS QSOs* can be recognized through an intercomparison of their infrared and polarization properties. Table 3 (updated from Hines & Schmidt 1997) examines the observed, or *apparent*, $\log(L_{IR}/L_{opt})$ and degree of polarization of the various samples. In each of these quantities the *IRAS*-QSOs stand out as extreme compared with optically-selected QSOs, with the BALQSOs forming an intermediate group. The very large values of $\log(L_{IR}/L_{opt})$ observed for the *IRAS*-QSOs are due to attenuation of optical

light, not an excess in the IR. Indeed, *IRAS*-QSOs appear no more IR-luminous than energetic non-*IRAS*-selected QSOs, and have typical *intrinsic* $\log(L_{IR}/L_{opt})$ after their optical luminosities are corrected for extinction (Hines et al. 1995, 1998b; Wills & Hines 1997). These objects would thus be indistinguishable from typical luminous QSOs if viewed from a direction of less obscuration (i.e., from the vantage point of the scattering material). The apparent $\log(L_{IR}/L_{opt})$ therefore is probably a good indicator of attenuation of UV/optical light in our direction. Within the dusty torus model, $\log(L_{IR}/L_{opt})$ correlates with inclination (e.g. Hines 1994); the degree of polarization behaves similarly due to both less dilution from unpolarized direct light and increased scattering angles.

While pure orientation provides an attractive explanation for these results, it would be naive to assume that evolutionary affects were not present (e.g., Sanders et al. 1988; Sanders & Mirabel 1996). The *IRAS*-QSOs tend to be in strongly interacting systems (Hutchings & Neff 1988; Surace et al. 1996; Hines et al. 1998a); recent *HST* imaging has revealed tidal structures as well as crowded immediate environments associated with the host galaxies of some classical low-z QSOs (e.g., Bahcall et al. 1997; Boyce et al. 1998). Both the epoch and vigor of a gravitational interaction presumably play into the characteristics of any structure which develops in the vicinity of the galactic nucleus, so encounters may well be important throughout the life of a QSO. It will be exciting to test these ideas and disentangle evolution from orientation with larger samples of *IRAS*-QSOs and improved far-IR photometry of BALQSOs, both of which can be provided by surveys with *SIRTF* and *NGST*.

We are grateful to several collaborators who assisted with the observations and engaged in discussions over the years: R.W. Goodrich, P.S. Smith, H.S. Stockman, B.J. Wills, and D. Wills. Investigations into the relationships between the polarimetric and infrared properties of AGN at Steward Observatory are supported by NSF grant AST-91-14087 and NASA grant NAG 5-3359.

REFERENCES

Antonucci, R. 1993, ARA&A, 31, 473

Antonucci, R.R.J., & Miller, J.S. 1985, ApJ, 297, 621

Bahcall, J.N., Kirhakos, S., Saxe, D.H., & Schneider, D.P. 1997, ApJ, 479, 642

Becker, R.H. et al. 1997, in Mass Ejection from AGN, ASP Conf. Series vol. 128, N. Arav, I. Shlosman, & R.J. Weymann, eds., 31

Berriman, G., Schmidt, G.D., West, S.C., & Stockman, H.S. 1990, ApJS, 74, 869

Blandford, R.D., & Lee, H.-W. 1997, in Mass Ejection from AGN, ASP Conf. Series vol. 128, N. Arav, I. Shlosman, & R.J. Weymann, eds., 88

Boroson, T.A., & Meyers, K.A. 1992, ApJ, 397, 442

Boyce, P.J., Disney, M.J., Blades, J.C., Boksenberg, A., Crane, P., Deharveng, J.M., Macchetto, F.D., Mackay, C.D. & Sparks, W.B. 1998, MNRAS, 298, 121

Breger, M. 1977, ApJ, 215, 119

Brotherton, M.S., Tran, H.D., Van Breugel, W., Dey, A., & Antonucci, R. 1997, ApJ, 487, L113

Brotherton, M.S., Van Breugel, W., Smith, R.J., Boyle, B.J., Shanks, T., Croom, S.M., Miller, L., & Becker, R.H. 1998, ApJ, 505, L7

Brown, J.C., & McLean, I.S. 1977, A&A, 57, 141

Cohen, M.H., Ogle, P.M., Tran, H.D., Vermeulen, R.C., Miller, J.S., Goodrich, R.W., & Martel, A.R. 1995, ApJ, 448, L77

Cutri, R.M., Huchra, J.P., Low, F.J., Brown, R.L., Vanden Bout, P.A. 1994, ApJ, 424, L65

Foltz, C.B., Chaffee, F.H., Weymann, R.J., & Morris, S.L. 1990, BAAS, 22, 806

Glenn, J., Schmidt, G.D., & Foltz, C.B. 1994, ApJ, 434, L47

Goodrich, R.W. 1997a, ApJ, 474, 606

_____. 1997b, in Mass Ejection from AGN, ASP Conf. Series vol. 128, N. Arav, I. Shlosman, & R.J. Weymann, eds., 88

Goodrich, R.W., & Miller, J.S. 1995, ApJ, 448, L73

Hamann, F., Korista, K.T., & Morris, S.L. 1993, ApJ, 415, 541

Hines, D.C. 1994, Ph.D. Thesis, Univ. of Texas at Austin

Hines, D.C., Low, F.J., Evans, A.S., Scoville, N.Z., Rieke, M., Thompson, R.I., & Schneider, G. 1998a, in preparation

Hines, D.C., & Schmidt, G.D. 1997, in Mass Ejection from AGN, ASP Conf. Series vol. 128, N. Arav, I. Shlosman, & R.J. Weymann, eds., 59

Hines, D.C., Schmidt, G.D., Smith, P.S., Cutri, R., & Low, F.J. 1995, ApJ, 450, L1

Hines, D.C., Schmidt, G.D., Wills, B.J., Smith, P.S., & Sowinski, G. 1998b, ApJ, in press

Hines, D.C., & Wills, B.J. 1993, ApJ, 415, 82

_____. 1995, ApJ, 448, L69

Hines, D.C., Wills, B.J., Schmidt, G.D., Sitko, M., Smith, P.S., Allen, R.G., & Goodrich, R.W. 1998c, in preparation

Hutchings, J.B., & Neff, S.G. 1988, AJ, 96, 1575

Jaffe, W., Ford, H., Ferrarese, L., van den Bosch, F., & O'Connell, R.W. 1996, ApJ, 460, 214

Korista, K.T., Voit, G.M., Morris, S.L., & Weymann, R.J. 1993, ApJS, 88, 357

Krolik, J.H., & Voit, G.M. 1998, ApJ, 497, L5

Low, F.J., Cutri, R.M., Kleinmann, S.G., & Huchra, J.P. 1989, ApJ, 340, L1

Low, F.J., & Hines, D.C. 1998, in Astrophysics with Infrared Surveys: A Prelude to *SIRTF*

Low, F.J., Huchra, J.P., Kleinmann, S.G., & Cutri, R.M. 1988, ApJ, 327, L41

Lynds, C.R. 1967, ApJ, 147, 396

Macchetto, F., Capetti, A., Sparks, W.B., Axon, D.J., & Boksenberg, A. 1994, ApJ, 435, L15

McIntosh, D.H., Rieke, M.J., Rix, H.-W., Foltz, C.B., and Weymann, R.J. 1998, preprint

Moore, R.L., & Stockman, H.S. 1984, ApJ, 279, 465

Ogle, P.M. 1997, in Mass Ejection from AGN, ASP Conf. Series vol. 128, N. Arav, I. Shlosman, & R.J. Weymann, eds., 78

_____. 1998, Ph.D. Thesis, Caltech

Sanders, D.B., & Murabel, I.F. 1996, ARA&A, 34, 749

Sanders, D.B., Soifer, B.T., Elias, J.H., Madore, B.F., Matthews, K., Neugebauer, G., & Scoville, N.Z. 1988, ApJ, 325, 74

Scargle, J.D., Caroff, L.J., & Noerdlinger, P.D. 1970, ApJ, 161, L115

Schmidt, G.D., Elston, R., & Lupie, O.L. 1992, AJ, 104, 1563

Schmidt, G.D., Hines, D.C., & Smith, P.S. 1997, in Mass Ejection from AGN, ASP Conf. Series vol. 128, N. Arav, I. Shlosman, & R.J. Weymann, eds., 106

Schmidt, G.D., Stockman, H.S., & Smith, P.S. 1992, ApJ, 398, L57

Schmidt, M. & Green, R.F. 1983, ApJ, 269, 352

Simmons, J.F.L., & Stewart, B.G. 1985, A&A, 142, 100

Smith, P.S., Schmidt, G.D., Allen, R.G., & Angel, J.R.P. 1995, ApJ, 444, 146

Sowinski, L.G., Schmidt, G.D., & Hines, D.C. 1997, in Mass Ejection from AGN, ASP Conf. Series vol. 128, N. Arav, I. Shlosman, & R.J. Weymann, eds., 305

Sprayberry, D., & Foltz, C.B. 1992, ApJ, 390, 39

Stocke, J.T., Morris, S.L., Weymann, R.J., & Foltz, C.B. 1992, ApJ, 396, 487

Stockman, H.S., & Angel, J.R.P. 1978, ApJ, 220, L67

Stockman, H.S., Angel, J.R.P., & Hier, R.G. 1981, ApJ, 243, 404

Storchi-Bergmann, T., Wilson, A.S., & Baldwin, J.A. 1992, ApJ, 396, 45

Surace, J.A., Sanders, D.B., Vacca, W.D., Veilleux, S., & Mazzarella, J.M. 1998, ApJ, 492, 116

Turnshek, D.A. 1988, in QSO Absorption Lines: Probing the Universe, ed. J.C. Blades, D. Turnshek, & C. Norman, STScI Symp. Ser. 2, (Cambridge: Cambridge Univ. Press), 17

Turnshek, D.A., Lupie, O.L., Rao, S.M., Espey, B.R., & Sirola, C.J. 1997a, ApJ, 485, 100

Turnshek, D.A., Monier, E.M., Sirola, C.J., & Espey, B.R. 1997b, ApJ, 476, 40

Voit, G.M., Weymann, R.J., & Korista, K.T. 1993, ApJ, 413, 95

Wardle, J.F.C., & Kronberg, P.P. 1974, ApJ, 194, 249

Weymann, R.J. 1997, in Mass Ejection from AGN, ASP Conf. Series vol. 128, N. Arav, I. Shlosman, & R.J. Weymann, eds., 3

Weymann, R.J., Morris, S.L., Foltz, C.B., & Hewitt, P.C. 1991, ApJ, 373, 23 (WMFH)

Wills, B.J., & Hines, D.C. 1997, in Mass Ejection from AGN, ASP Conf. Series vol. 128, N. Arav, I. Shlosman, & R.J. Weymann, eds., 99

Wills, B.J., Wills, D., Breger, M., Antonucci, R.R.J., & Barvainis, R. 1992a, ApJ, 398, 454

Wills, B.J., Wills, D., Evans, N.J., Natta, A., Thompson, K.L., Breger, M., & Sitko, M.L. 1992b, ApJ, 400, 96

Young, S., Hough, J.H., Efstathiou, A., Wills, B.J., Bailey, J.A., Ward, M.J., & Axon, D.J. 1996, MNRAS, 281, 1206

This preprint was prepared with the AAS LaTeX macros v4.0.

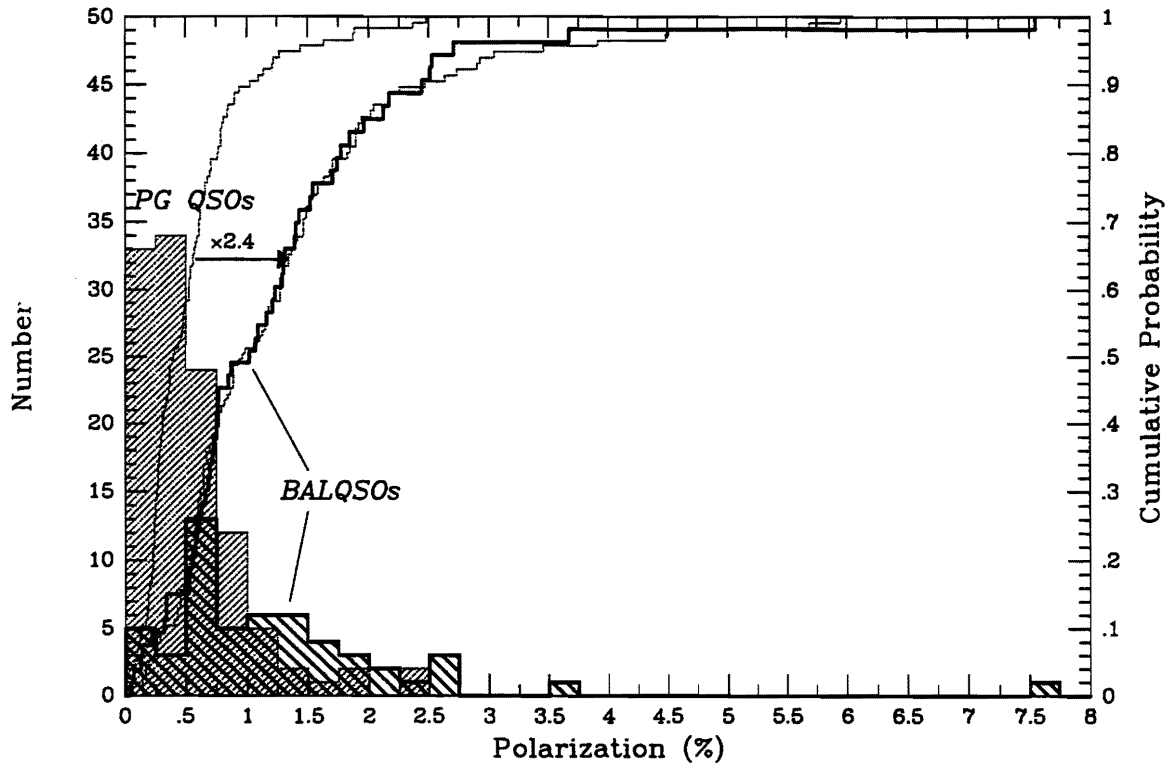

Fig. 1.— Differential and cumulative distributions of optical polarization for the 53-member BALQSO sample (heavy solid line and histogram) and the PG QSO catalog – an optical survey selected without regard for the presence of absorption lines (labeled light dashed line and histogram). The likelihood of the two observed samples being drawn from the same parent is less than 1 in 10^6. However, the two distributions can be made consistent if the polarization of each PG QSO is simply multiplied by a factor 2.4 (redrawn light line and arrow). This is equivalent to the BALQSO sample being a subset of all optically-selected QSOs, in which the direct nuclear light suffers, on average, ~1 mag of attenuation in our direction.

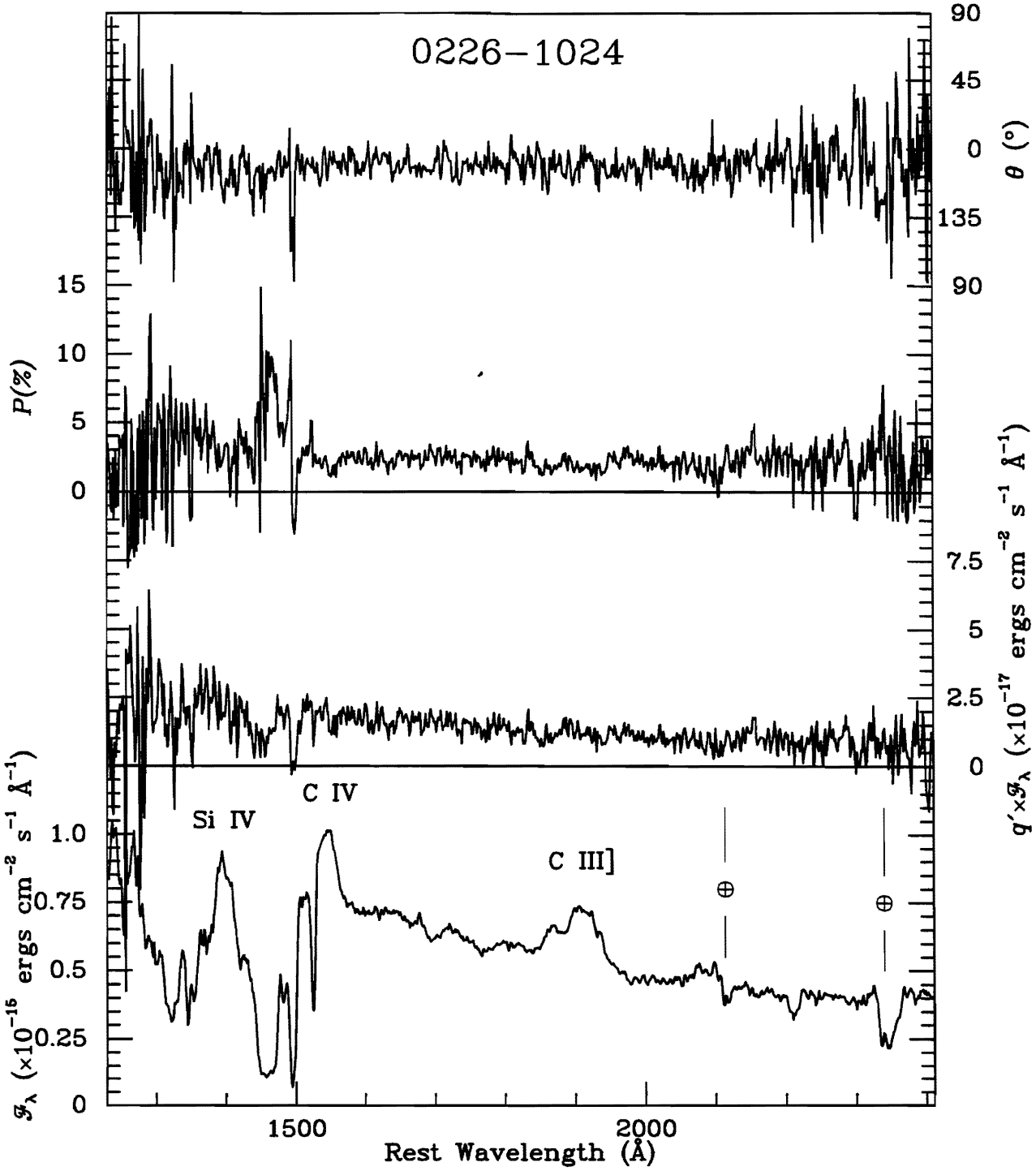

Fig. 2.— *Bottom to top:* Total flux, polarized flux, degree of polarization, and position angle for the BALQSO 0226−1024. The degree of polarization has been corrected for statistical bias due to the finite measurement uncertainties (Wardle & Kronberg 1974), hence P can occasionally fall below zero. Polarized flux, $q' \times F_\lambda$, is shown for a coordinate frame rotated to the position angle of overall polarization, thus it is unaffected by the positive bias which plagues P. Terrestrial absorption features are noted.

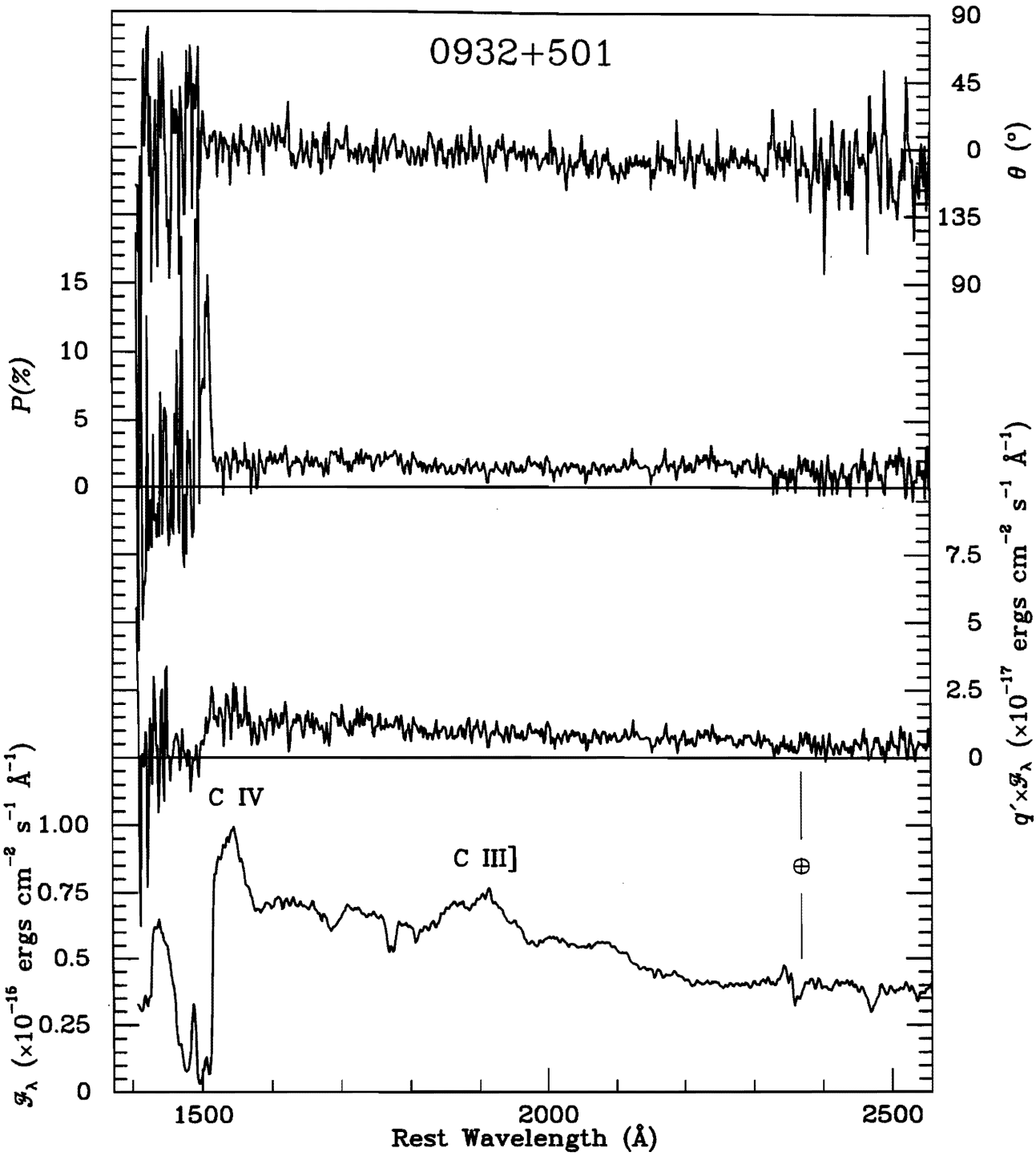

Fig. 3.— As in Fig. 2 for 0932+501.

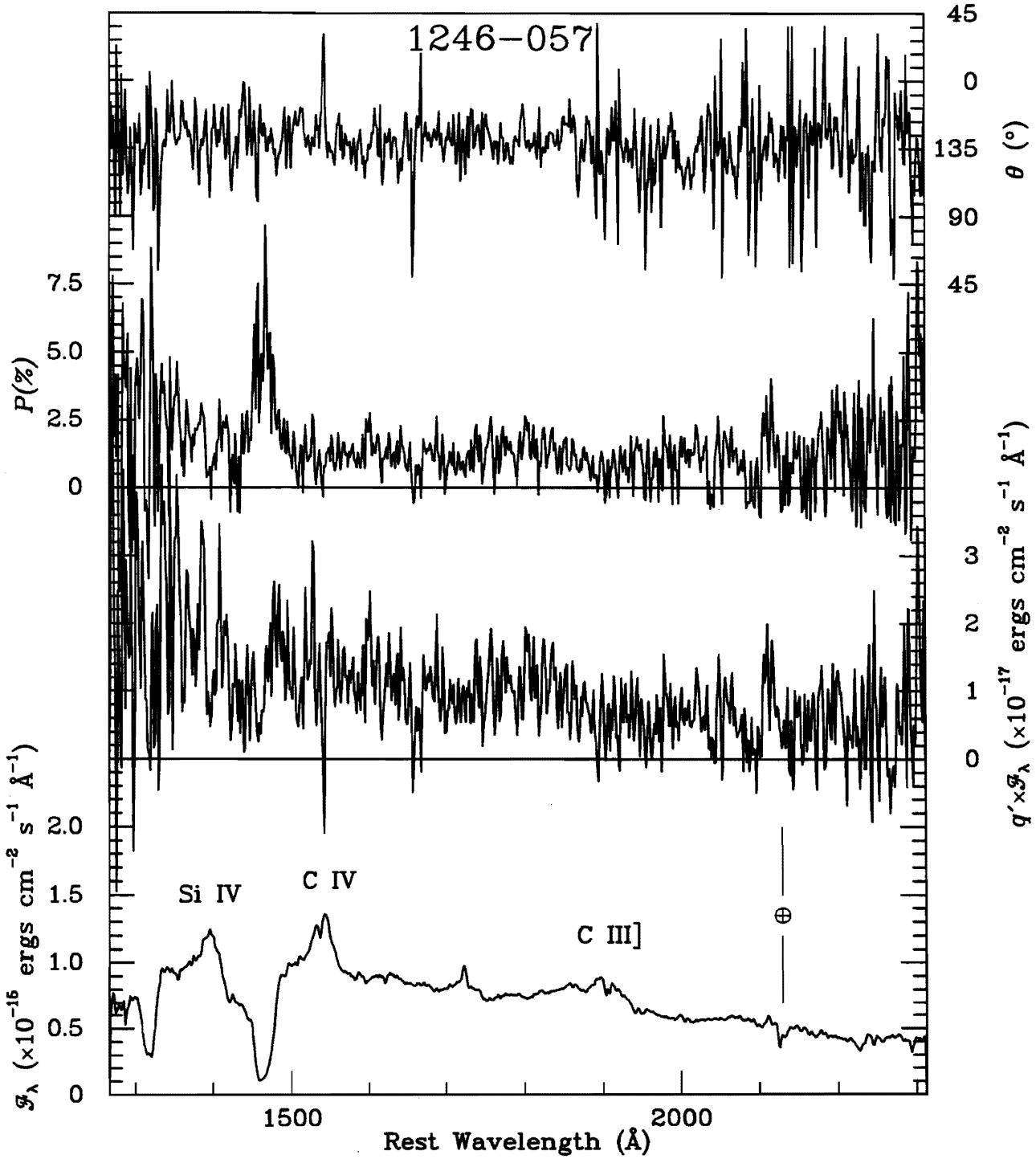

Fig. 4.— As in Fig. 2 for 1246−057.

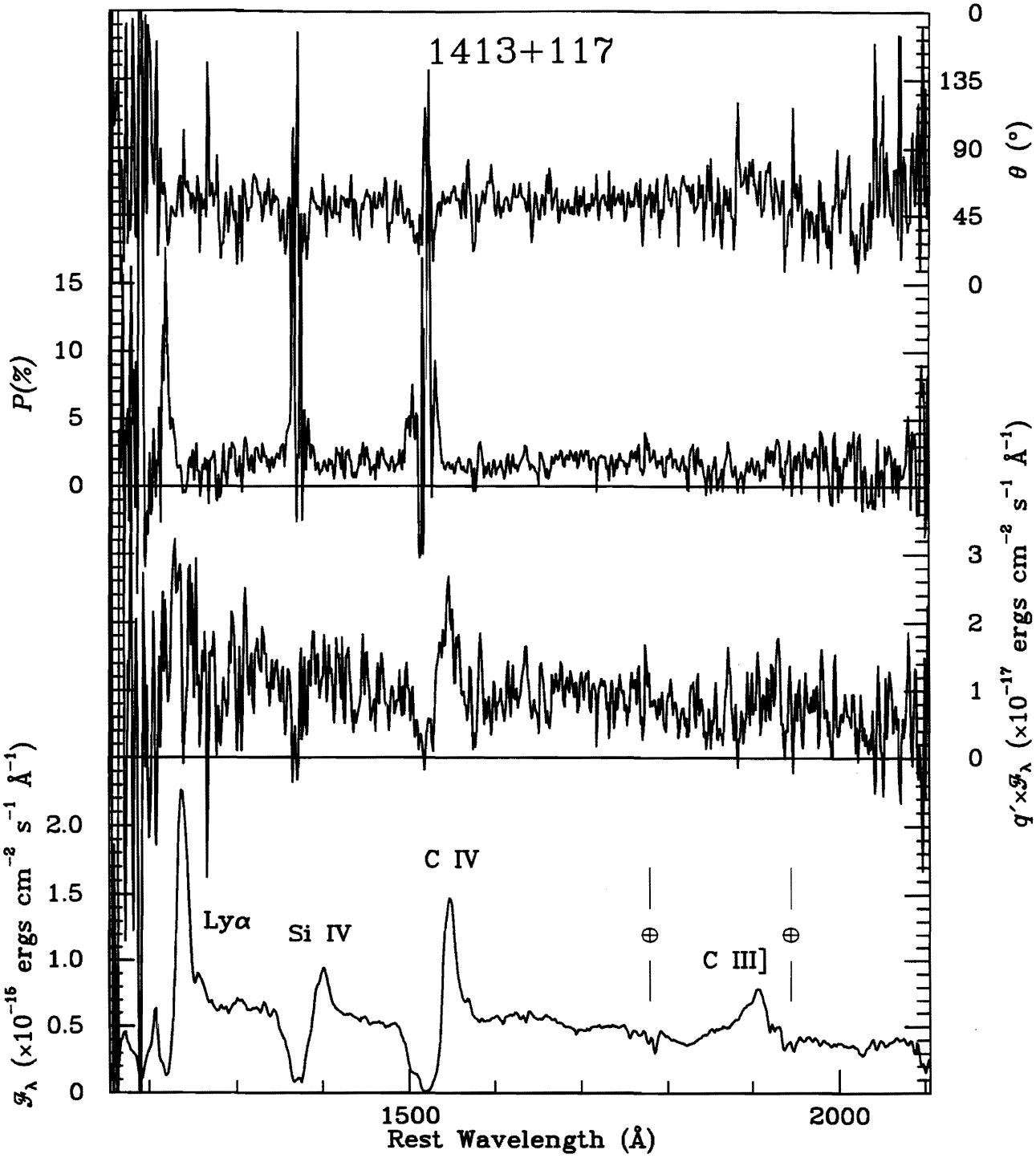

Fig. 5.— As in Fig. 2 for 1413+117.

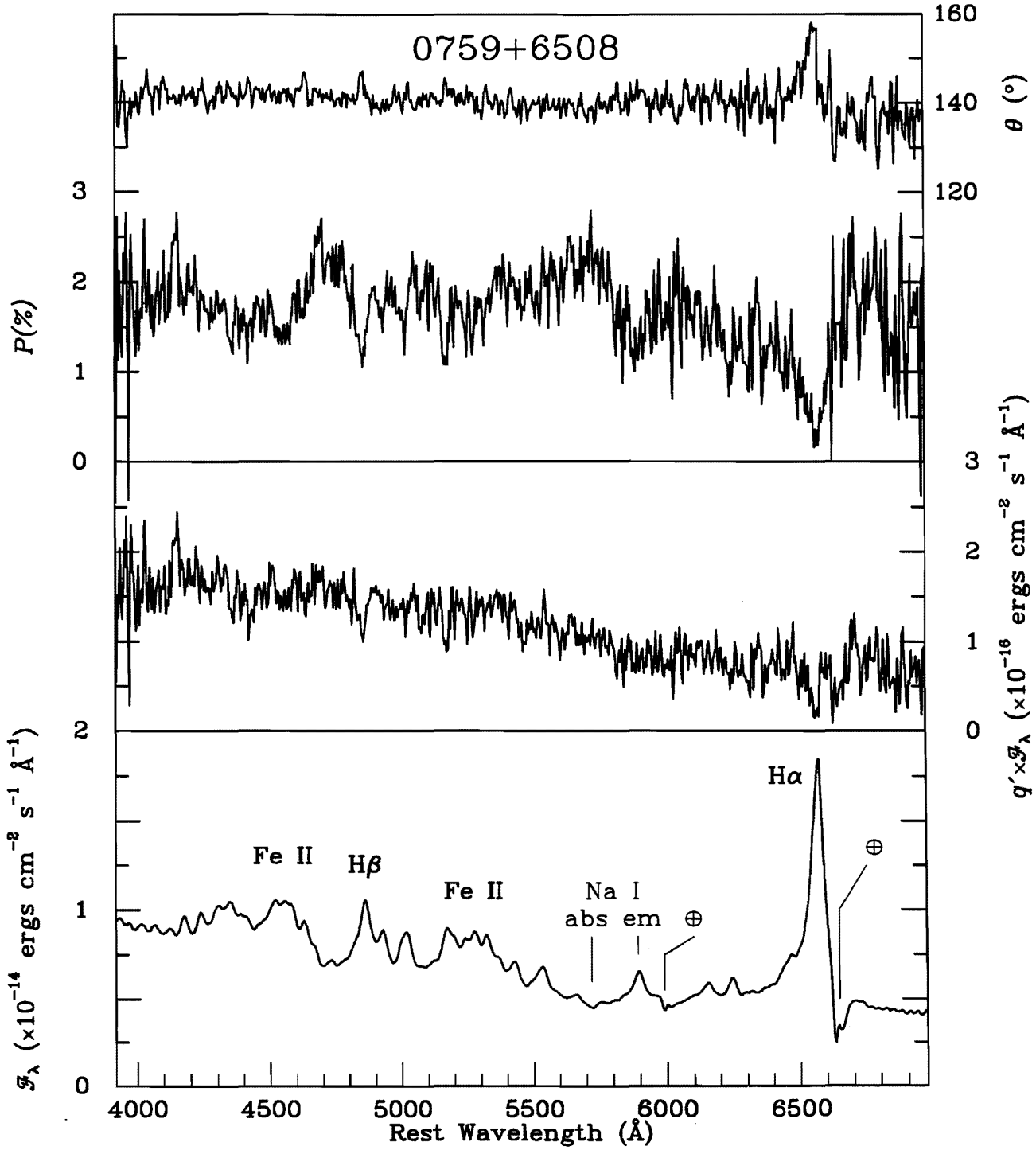

Fig. 6.— As in Fig. 2 for 0759+6508. As in Fig. 2 for 0759+6508. The emission and absorption features associated with Na I D are noted.

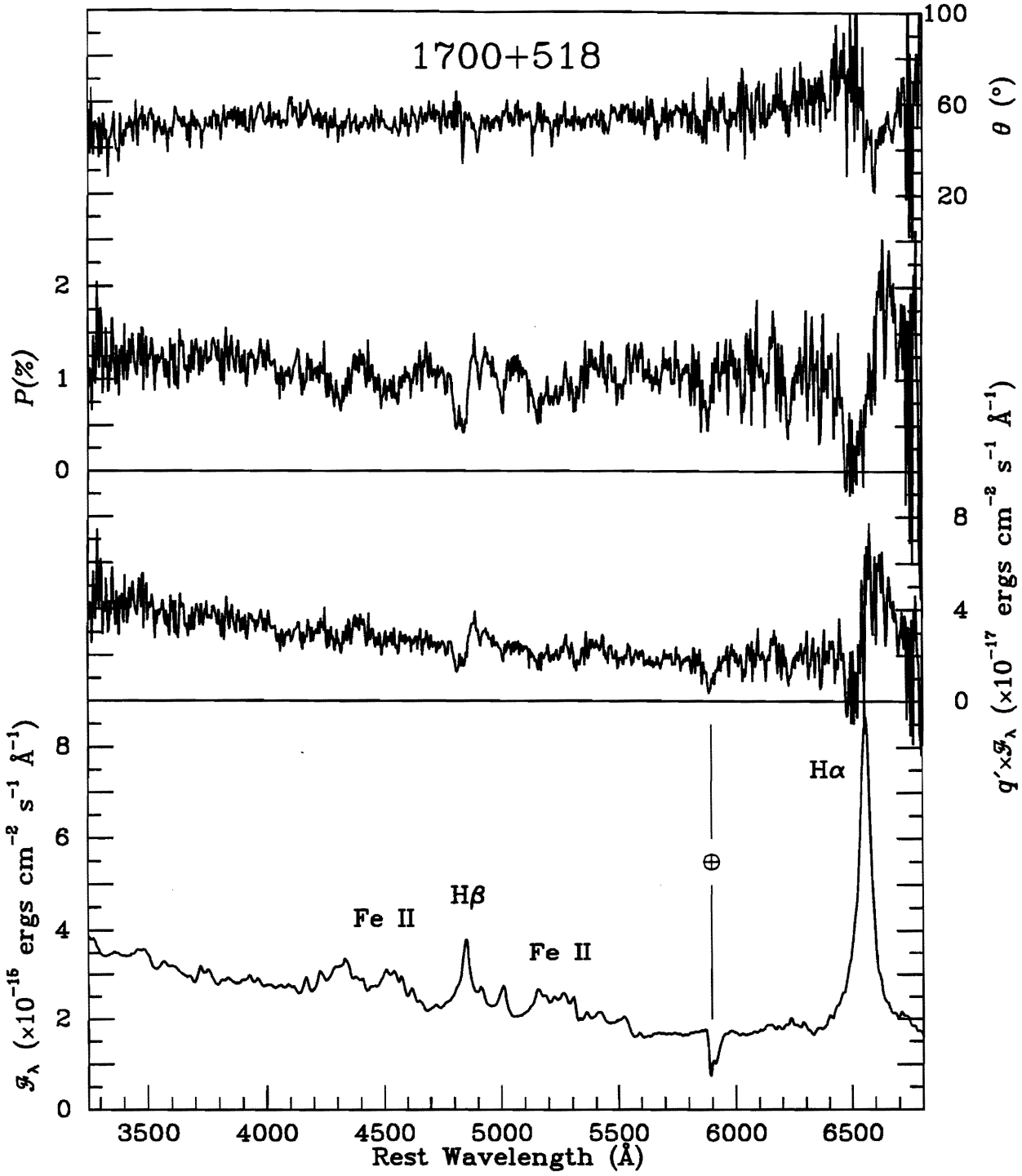

Fig. 7.— As in Fig. 2 for 1700+518.

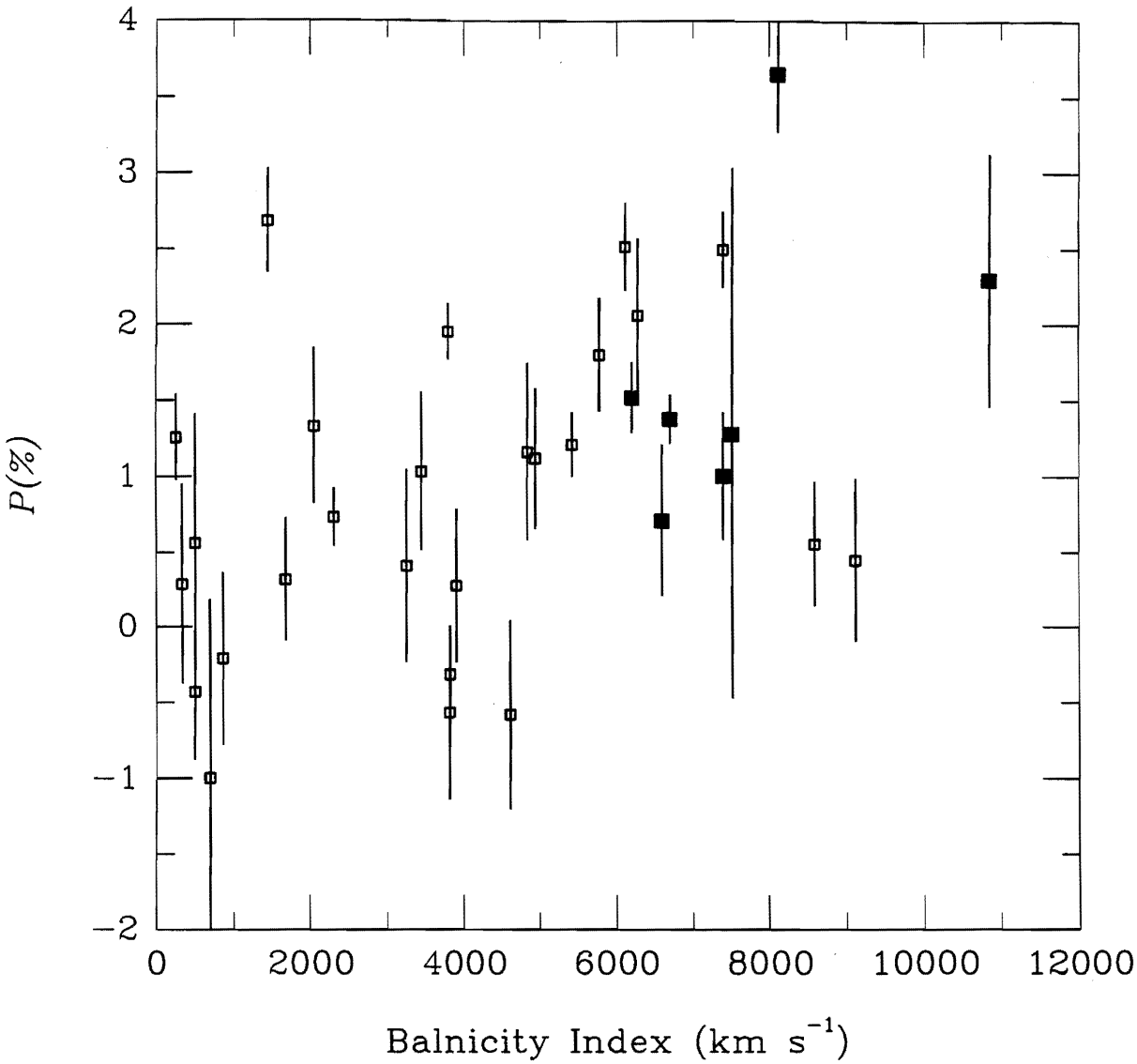

Fig. 8.— Relation between degree of polarization and C IV λ1550 balnicity index. Low-ionization BALQSOs are shown as filled squares. P has been corrected for uncertainty bias and error bars are $\pm 1\sigma$.

Table 1. THE SURVEY

Object	z_{em}	Date (yyyymmdd)	Telescope	$\lambda\lambda$[a]	$P \pm \sigma_P$ (%)	$\theta \pm \sigma_\theta$ (°)
0004+0147	1.711	19890926	MO 2.1m	W	1.13 ± 0.40	117.7 ± 10.2
		19900923	SO 2.3m	W	1.45 ± 0.38	125.6 ± 7.4
		Sum		W	1.29 ± 0.28	122.3 ± 6.1
0010−0012	2.145	19890926	MO 2.1m	W	1.70 ± 0.77	115.7 ± 12.9
0013+0138	1.665	19901117	SO 2.3m	W	0.34 ± 0.94	110.3 ± 52.0
0018+0047	1.835	19901117	SO 2.3m	W	0.88 ± 0.79	107.7 ± 25.8
		19910910	SO 2.3m	W	1.48 ± 1.23	155.5 ± 23.8
		Sum		W	0.72 ± 0.66	126.0 ± 26.4
0019+0107	2.124	19781105	KPNO 4m	W	0.93 ± 0.26	24.0 ± 8.0
		19800114	SO 2.3m	W	1.38 ± 0.65	44.0 ± 14.0
		19890928	MO 2.1m	W	0.44 ± 0.31	21.4 ± 20.0
		Sum		W	0.76 ± 0.19	26.3 ± 7.2
0020−0154	1.46	19890927	MO 2.1m	W	0.34 ± 0.90	171.6 ± 52.0
0021−0213	2.348	19890928	MO 2.1m	W	0.95 ± 0.94	27.0 ± 28.5
		19900925	SO 2.3m	W	0.91 ± 0.82	128.7 ± 25.6
		Sum		W	0.22 ± 0.62	153.4 ± 52.0
0025−0151	2.076	19890926	MO 2.1m	W	1.02 ± 0.95	98.7 ± 26.7
		19900925	SO 2.3m	W	1.26 ± 0.63	112.6 ± 14.3
		Sum		W	1.16 ± 0.52	109.0 ± 13.0
0029+0017	2.253	19890927	MO 2.1m	W	1.20 ± 1.09	3.2 ± 25.9
		19900923	SO 2.3m	W	1.53 ± 0.68	152.5 ± 12.6
		Sum		W	1.30 ± 0.58	159.1 ± 12.8
0043+008	2.137	19781104	KPNO 4m	W	0.33 ± 0.38	103.0 ± 33.0
		19901118	SO 2.3m	W	1.00 ± 0.62	11.3 ± 17.7
		Sum		W	0.04 ± 0.32	179.8 ± 52.0
0051−0019	1.713	19901015	MO 2.1m	W	1.04 ± 1.16	84.7 ± 32.0
		19901018	MO 2.1m	W	0.68 ± 0.76	101.6 ± 32.2
		Sum		W	0.76 ± 0.64	95.0 ± 24.1
0054+0200	1.872	19901016	MO 2.1m	W	1.03 ± 1.76	81.5 ± 49.1
		19901117	SO 2.3m	W	1.04 ± 0.97	69.6 ± 26.6
		Sum		W	1.02 ± 0.85	72.3 ± 23.8
0059−0206	1.321	19890925	MO 2.1m	W	1.15 ± 0.44	150.9 ± 10.9
		19900925	SO 2.3m	W	1.01 ± 0.95	62.4 ± 27.1
		Sum		W	0.77 ± 0.40	150.6 ± 14.9
0059−2735	1.593	19941109	SO 1.5m	W	2.44 ± 0.83	169.1 ± 9.7

Table 1—Continued

Object	z_{em}	Date (yyyymmdd)	Telescope	$\lambda\lambda$[a]	$P \pm \sigma_P$ (%)	$\theta \pm \sigma_\theta$ (°)
0109−014	1.758	19901015	MO 2.1m	W	1.83 ± 0.36	76.8 ± 5.6
		19901017	MO 2.1m	U+B+V	0.95 ± 1.34	65.8 ± 40.4
		Sum		W	1.77 ± 0.35	76.4 ± 5.6
0117−180	1.790	19901117	SO 2.3m	W	1.40 ± 0.46	12.6 ± 9.5
0137−018	2.232	19901118	SO 2.3m	W	0.58 ± 0.51	28.3 ± 25.4
0145+042	2.029	19811022	SO 2.3m	W	0.57 ± 0.69	131.0 ± 34.7
		19900925	SO 2.3m	W	1.80 ± 0.62	150.0 ± 9.9
		Sum		W	1.21 ± 0.46	146.3 ± 11.0
0146+017	2.909	19781106	KPNO 4m	W	1.17 ± 0.23	138.0 ± 6.0
		19800114	SO 2.3m	W	2.44 ± 0.89	139.0 ± 10.0
		19901015	MO 2.1m	W	1.37 ± 0.60	157.4 ± 12.5
		Sum		W	1.23 ± 0.21	140.5 ± 4.9
0226−1024	2.256	19900923	SO 2.3m	W	2.51 ± 0.25	165.4 ± 2.9
0254−334	1.863	19811024	SO 2.3m	W	0.63 ± 1.18	154.0 ± 52.0
0335−336	2.258	19900923	SO 2.3m	W	2.17 ± 1.75	14.3 ± 23.1
0759+6508	0.148	...	MO 2.1m	W[b]	1.52 ± 0.14	117.8 ± 2.7
		19951025	SO 2.3m	R	1.45 ± 0.14	119.0 ± 2.8
0856+172	2.131	19821213	SO 2.3m	W	2.60 ± 1.60	74.0 ± 18.0
		19841029	SO 2.3m	W	4.00 ± 1.50	17.0 ± 10.0
		19850121	SO 2.3m	W	1.00 ± 0.50	1.0 ± 16.0
		19901118	SO 2.3m	W	0.71 ± 0.95	101.6 ± 38.3
		Sum		W	0.69 ± 0.41	9.7 ± 17.0
0903+175	2.776	19821214	SO 2.3m	W	0.70 ± 0.54	21.0 ± 22.0
0932+501	1.914	19821214	SO 2.3m	W	1.53 ± 0.21	167.0 ± 4.0
		19830308	SO 1.5m	W	1.51 ± 0.34	167.0 ± 6.0
		19890923	MO 2.1m	W	0.92 ± 0.34	159.7 ± 10.6
		Sum		W	1.39 ± 0.16	166.0 ± 3.3
0946+301	1.216	19830607	SO 2.3m	W	0.79 ± 0.19	110.0 ± 7.0
		19890923	MO 2.1m	W	0.98 ± 0.22	123.3 ± 6.4
		Sum		W	0.85 ± 0.14	116.4 ± 4.9
1011+091	2.266	19821214	SO 2.3m	W	0.99 ± 0.40	101.0 ± 11.0
		19890408	MO 2.1m	W	2.71 ± 0.49	145.2 ± 5.2
		19901118	SO 2.3m	W	1.55 ± 0.45	139.8 ± 8.2
		19950427	SO 1.5m	W	2.40 ± 0.51	139.5 ± 6.1
		Sum		W	1.54 ± 0.23	135.9 ± 4.2

Table 1—Continued

Object	z_{em}	Date (yyyymmdd)	Telescope	$\lambda\lambda$[a]	$P \pm \sigma_P$ (%)	$\theta \pm \sigma_\theta$ (°)
1013+1126	2.22	19901118	SO 2.3m	W	1.07 ± 0.59	168.8 ± 15.9
1157+014	1.986	19780303	SO 2.3m	W	0.91 ± 0.61	30.0 ± 19.0
		19810202	SO 2.3m	W	0.51 ± 0.74	27.6 ± 41.6
		Sum		W	0.75 ± 0.47	29.3 ± 18.0
1208+1535	1.961	19900223	MO 2.1m	W	0.07 ± 0.57	155.7 ± 52.0
1214+1753	0.679	19890409	MO 2.1m	W	0.73 ± 0.43	171.4 ± 16.9
1228+1216	1.408	19890409	MO 2.1m	W	0.14 ± 0.45	77.7 ± 52.0
1246−057	2.236	19780404	SO 2.3m	W	1.91 ± 0.30	139.0 ± 5.0
		19790402	SO 2.3m	W	2.09 ± 0.33	159.0 ± 5.0
		19790402	SO 2.3m	U+B+V	3.89 ± 0.65	136.0 ± 5.0
		19790402	SO 2.3m	R+I	1.44 ± 0.43	136.0 ± 9.0
		19800114	SO 2.3m	W	2.10 ± 0.29	149.0 ± 4.0
		Sum		W	1.96 ± 0.18	148.7 ± 2.6
1254+047	1.024	19900923	MO 2.1m	W	0.61 ± 0.18	6.3 ± 8.6
1303+308	1.763	19810202	SO 2.3m	W	6.13 ± 2.42	73.1 ± 11.0
		19810204	SO 2.3m	W	1.28 ± 0.63	176.1 ± 14.0
		19950426	SO 1.5m	W	0.24 ± 0.56	173.7 ± 52.0
		Sum		W	0.52 ± 0.41	179.8 ± 22.6
1309−056	2.212	19780609	SO 2.3m	W	2.28 ± 0.52	179.3 ± 6.5
		19800114	SO 2.3m	W	1.53 ± 0.70	165.0 ± 13.0
		19810202	SO 2.3m	W	1.04 ± 0.85	179.7 ± 23.2
		19890409	MO 2.1m	W	3.80 ± 2.16	172.7 ± 16.9
		Sum		W	1.84 ± 0.37	175.8 ± 5.7
1331−0108	1.881	19950425	SO 1.5m	W	1.09 ± 0.42	19.1 ± 11.0
1402+4341	0.324	19880416	MO 2.1m	W[b]	8.04 ± 0.33	34.2 ± 1.2
		19880419	MO 2.1m	W[b]	7.22 ± 0.28	31.3 ± 1.1
		19950428	SO 1.5m	R	4.23 ± 0.36	28.2 ± 2.4
		19950428-9	SO 1.5m	B	9.39 ± 0.48	29.1 ± 1.5
		19950429	SO 1.5m	U	14.94 ± 0.87	30.2 ± 1.7
		Sum		W	7.55 ± 0.22	32.6 ± 0.8
1413+117	2.551	19810607	SO 2.3m	W	3.46 ± 0.50	49.0 ± 4.0
		19890407	MO 2.1m	W	2.10 ± 0.35	55.6 ± 4.9
		19890408	MO 2.1m	U+B+V	3.12 ± 0.64	49.9 ± 5.9
		19890408	MO 2.1m	R+I	1.63 ± 0.50	55.9 ± 8.9
		Sum		W	2.53 ± 0.29	52.7 ± 3.3

Table 1—Continued

Object	z_{em}	Date (yyyymmdd)	Telescope	$\lambda\lambda$[a]	$P \pm \sigma_P$ (%)	$\theta \pm \sigma_\theta$ (°)
1520+4123	3.1	19950426	SO 1.5m	W	1.74 ± 1.11	6.5 ± 18.3
1524+5147	2.873	19900925	SO 2.3m	W	2.71 ± 0.34	93.8 ± 3.6
1556+335	1.65	19900925	SO 2.3m	W	1.31 ± 0.47	70.2 ± 10.3
1700+518	0.292	19830608	SO 2.3m	W	0.54 ± 0.10	56.0 ± 5.0
		19950426	SO 1.5m	W	0.71 ± 0.15	53.3 ± 6.1
		19950426-8	SO 1.5m	V	0.73 ± 0.23	44.6 ± 8.9
		19950427	SO 1.5m	R	1.32 ± 0.36	50.5 ± 7.8
		19950427	SO 1.5m	I	0.61 ± 0.50	80.3 ± 23.5
		19950429	SO 1.5m	B	1.06 ± 0.21	52.2 ± 5.7
		Sum		W	0.59 ± 0.08	55.0 ± 4.0
2154−2005	2.035	19900923	SO 2.3m	W	0.53 ± 0.57	143.3 ± 29.0
2201−1834	1.814	19900923	SO 2.3m	W	1.43 ± 0.51	7.1 ± 10.2
2225−055	1.981	19781028	SO 2.3m	W	4.40 ± 0.65	167.0 ± 4.0
		19781105	KPNO 4m	W	3.30 ± 0.46	165.0 ± 5.0
		Sum		W	3.67 ± 0.38	165.8 ± 2.9
2233+134	0.325	19830830	SO 2.3m	W	0.56 ± 0.15	80.0 ± 8.0
2241+0016	1.394	19890925	MO 2.1m	W	0.66 ± 0.56	164.8 ± 24.5
		19900925	SO 2.3m	W	0.68 ± 0.54	174.5 ± 22.8
		Sum		W	0.66 ± 0.39	169.9 ± 16.8
2341−235	2.822	19830901	SO 2.3m	W	0.13 ± 0.46	28.0 ± 52.0
2348−011	3.014	19830830	SO 2.3m	W	0.32 ± 0.83	32.0 ± 52.0
2350−0045	1.617	19890925	MO 2.1m	W	0.63 ± 0.73	138.4 ± 33.1
		19900925	SO 2.3m	W	1.50 ± 0.70	96.6 ± 13.2
		Sum		W	0.87 ± 0.50	106.7 ± 16.7
2358+0216	1.872	19900925	SO 2.3m	W	2.12 ± 0.51	44.9 ± 6.9

[a]W = "white" light, $\sim\lambda\lambda 3200 - 8600$

[b]B. Wills, private communication

Table 2. POLARIMETRIC TRENDS AMONG BALQSOs

Object	z_{em}	Low-Ion. BALQSO?	$P_{\lambda 5500,\mathrm{obs}}$	$P_\lambda(\%)^a$	$P_{BEL}(\%)^a$	$P_{BAL}(\%)^a$
07598+6508[b,c]	0.15	√	2.5%	(↖)	↓	(↑)
1700+518[b]	0.29	√	1.0%	(↖)	(↓)	?
1402+4341[d]	0.32	√	7.6%	↖	(↓)	↑,↔
0840+3633[e]	1.22	√	2.5%	↖	↓	(↑)
0932+501[b]	1.91	√	1.5%	↖	↓	↑
PHL 5200[f,g,h]	1.98	√	5.0%	↖	↓	↑
1246−057[b]	2.23		1.3%	(↖)	↓	↑
0226−1024[b,i]	2.25		2.4%	↖	↓	↑,↔
1413+117[b,g]	2.55		1.5%	↖	(↓)	↑
CSO 755[j]	2.85		4.5%	↖	↓	↑,↔
0105−265[h]	3.52		2.0%	↖	↓	↑

[a] ↑ = increase; ↖ = increase to blue; ↓ = decrease; ↔ = no change; ( ) = marginal/complex.

References. — [b]this paper; [c]Hines & Wills (1995); [d]Hines et al. (1998c); [e]Brotherton et al. (1997); [f]Stockman et al. (1981); [g]Goodrich & Miller (1995); [h]Cohen et al. (1995); [i]Ogle (1997); [j]Glenn et al. (1994)

Table 3. OBSERVED PROPERTIES for non-BALQSOs, BALQSOs and *IRAS*-QSOs

Class	Median $P(\%)$ (range)	$\langle L_{\mathrm{IR}}/L_{\mathrm{opt}}\rangle$ (range)
non-BALQSOs	0.4% (0.1%–2.5%)	7 (0.3–17)
BALQSOs	1.0% (0.1%–7.6%)	11 (7–17)
IRAS-QSOs	2.7% (0.1%–16.4%)	199 (48–370)